

Reductive Cleavage Mechanism of Methylcobalamin: Elementary Steps of Co–C Bond Breaking

Pawel M. Kozlowski,^{*,†} Jadwiga Kuta,[†] and Włodzimierz Galezowski[‡]

Department of Chemistry, University of Louisville, Louisville, Kentucky 40292, and Department of Chemistry, A. Mickiewicz University, Grunwaldzka 6, 60-780 Poznań, Poland

Received: October 24, 2006; In Final Form: March 15, 2007

Density functional theory has been applied to the investigation of the reductive cleavage mechanism of methylcobalamin (MeCbl). In the reductive cleavage of MeCbl, the Co–C bond is cleaved homolytically, and formation of the anion radical $[\text{MeCbl}]^{\bullet-}$ reduces the dissociation energy by $\sim 50\%$. Such dissociation energy lowering in $[\text{MeCbl}]^{\bullet-}$ arises from the involvement of two electronic states: the initial state, which is formed upon electron addition, has dominant π^*_{corrin} character, but when the Co–C bond is stretched the unpaired electron moves to the $\sigma^*_{\text{Co-C}}$ state, and the final cleavage involves the three-electron $(\sigma)^2(\sigma^*)^1$ bond. The $\pi^*_{\text{corrin}}-\sigma^*_{\text{Co-C}}$ states crossing does not take place at the equilibrium geometry of $[\text{MeCbl}]^{\bullet-}$ but only when the Co–C bond is stretched to 2.3 Å. In contrast to the neutral cofactor, the most energetically efficient cleavage of the Co–C bond is from the base-off form. The analysis of thermodynamic and kinetic data provides a rationale as to why Co–C cleavage in reduced form requires prior departure of the axial base. Finally, the possible connection of present work to B₁₂ enzymatic catalysis and the involvement of anion–radical-like $[\text{MeCbl}]^{\bullet-}$ species in relevant methyl transfer reactions is discussed.

1. Introduction

The question of how B₁₂-dependent enzymes activate and subsequently facilitate cleavage of the Co–C bond remains one of the most important and poorly understood aspects of B₁₂ enzymatic catalysis.¹ These enzymes are distinguished by the specific forms of the B₁₂ cofactors (Figure 1) that support distinctive chemical pathways: (1) Enzymes that utilize methylcobalamin (MeCbl) to catalyze methyl transfer reactions² in which the Co–C bond appears to be heterolytically cleaved³ and (2) enzymes that employ adenosylcobalamin (AdoCbl) to catalyze organic rearrangement reactions in which the first step involves the homolytic cleavage of the Co–C bond.⁴ Much effort (both experimental and theoretical) has been devoted toward the understanding of how Co–C reactivity can be directed so differently in MeCbl- and AdoCbl-dependent enzymes. In particular, the mechanism by which the spectacular 10¹²-fold rate enhancement⁵ of the Co–C homolysis step is achieved by AdoCbl-dependent enzymes remains to be fully explained.

Both cofactors possess a relatively weak Co–C bond, and its strength must be significantly lowered during enzymatic catalysis. In AdoCbl-dependent enzymes the dissociation energy of the Co–C bond, which in solution is ~ 32 kcal/mol,^{5,6} must be reduced by $\sim 50\%$ to achieve the 10¹²-fold rate enhancement. Although the origin of such enormous catalytic activity remains unexplained, the Co–C bond weakening by one-electron reduction (or oxidation) has generated considerable interest.^{7–11} The one-electron reduction can be accomplished electrochemically as was first demonstrated by Lexa and Savéant.⁷ More recently, electroreduction of a series of alkylcobalamins and an analysis of solvent effect were reported by Birke and co-

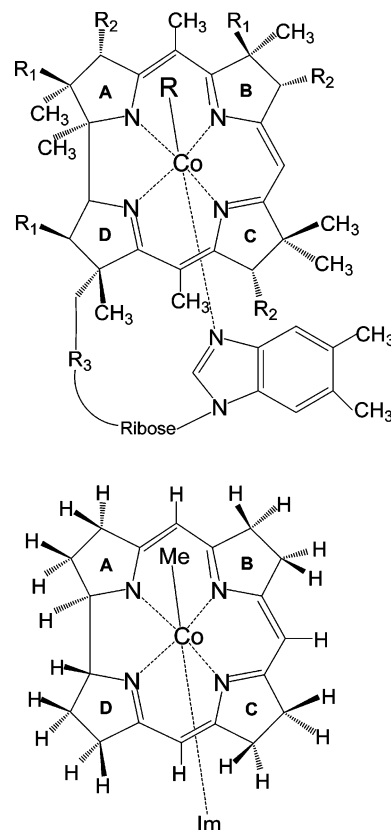


Figure 1. Molecular structure of B₁₂ cofactors (top panel) where R = Me for MeCbl and R = Ado for AdoCbl (R₁ = CH₂CONH₂, R₂ = CH₂CH₂CONH₂, R₃ = (CH₂)₂CONHCH₂CH(CH₃)OPO₃[−]). The bottom panel shows the structural model of MeCbl employed in the present study and is denoted as Im–[Co^{III}(corrin)]–Me⁺.

workers.^{10,11} In the reductive cleavage of MeCbl the Co–C bond is homolytically cleaved, and formation of a radical anion

* To whom correspondence should be addressed. Tel: +1 502 852-6609, Fax: +1 502 852-8149, E-mail: pawel@louisville.edu.

[†] University of Louisville.

[‡] A. Mickiewicz University.

([MeCbl]^{•−}) enormously enhances the rate of Co–C bond dissociation. Martin and Finke¹² estimated that the dissociation energy of the Co–C bond can be lowered by 68% (more specifically only 58%¹³) and the homolysis rate can be enhanced by a factor of $\sim 10^{15}$ when the cleavage of the Co–C bond involves the reduced form of cofactor.

Despite the importance and potential relevance to B₁₂ enzymatic catalysis, the mechanism of reductive cleavage remains essentially unexplained. Originally, Martin and Finke¹² suggested that the observed rate enhancement is due to “half”-strength of the Co–C bond, which implies that the addition of an electron leads to a radical anion in which the σ^* molecular orbital (MO) of Co–C is populated, thereby forming a three-electron (or net “one”-electron) bond. Such direct electron transfer into the σ^* LUMO has been recently postulated for the reductive cleavage of disulfides.¹⁴ However, for the systems containing a corrin ring, this simple MO picture is not supported by any calculations that are published to date. Three decades ago, Salem et al.¹⁵ showed in a structural model of MeCbl that the LUMO orbital has a π^* _{corrin} character. More recently, density functional theory (DFT)^{16,17} calculations have also revealed that the Co–C σ^* MO is located energetically higher than the LUMO and is additionally separated by other MOs. This implies that addition of an extra electron would generate an intermediate that has corrin π -anion-radical character. Furthermore, the reductive cleavage mechanism must involve an interaction of two electronic states, which have dominant π^* _{corrin} and σ^* _{Co–C} character, and it is not immediately obvious how these two electronic states should interact to reduce the Co–C bond dissociation energy. Birke et al.^{10,11} performed DFT calculations on models of one-electron reduced cobalamins to explore the possibility of such an interaction. They argue that the single-configuration ground-state DFT calculations show a large separation between the energy of the SOMO (which has π^* _{corrin} character) and the σ^* _{Co–C}. This energy gap appears to be too large for the intramolecular electron transfer to give the fast kinetics that is observed according to the semi-classical theory of Savéant.¹⁸ To provide further insight, Spataru and Birke¹⁹ used a multi-configurational CASSCF method to explore the mechanism of reductive Co–C bond cleavage. They argued that such an approach is necessary because previously reported DFT calculations did not show any change in the Co–C bond distance for the anion radical. The lack of evident structural changes was attributed by these authors to “failure of the conventional DFT method”.²⁰ Consequently, they used different active spaces in CASSCF calculations and obtained, when the active space was extended by the σ^* MO of Co–C, strong mixing of the states that caused an increase in the Co–C bond length. Finally, a possibility of the pseudo Jahn–Teller (pJT) effect was invoked as a reason for a reduced energy gap between the π^* _{corrin} and the σ^* _{Co–C} states.

The above summary shows that the origin of the Co–C bond dissociation lowering in [MeCbl]^{•−} is not yet fully understood. In the present study we use density functional theory (DFT) to explore the reductive cleavage mechanism. To accomplish this it is necessary to know low-lying excited states that would be obtained using time-dependent DFT (TD–DFT).^{21,22} These newly obtained results shed considerable new light on the mechanism of reductive Co–C bond cleavage and rationalize the significant lowering of the dissociation energy.

2. Method of Calculation

All of the calculations reported in this work were carried out using nonlocal DFT with the nonhybrid Becke–Perdew (BP86)²³

TABLE 1: Axial Bond Lengths^a

system	Co–C (Å)	Co–N _{ax} (Å)
Im–[Co ^{III} (corrin)]–Me ⁺	1.968	2.132
[Co ^{III} (corrin)]–Me ⁺	1.946	
Im–[Co ^{II} (corrin)] ⁺		2.094
Im–[Co ^{III} (corrin [•])]–Me	1.958	2.112
[Co ^{III} (corrin [•])]–Me	1.932	

^a Optimized at the BP86/6-31G(d) level of theory.

functional and the 6-31G(d) basis set (5d components) as implemented in the Gaussian²⁴ suite of programs for electronic structure calculations. This level of theory was found to be appropriate for structural analysis and for electronic properties^{25–30} (including low-lying electronically excited states¹⁷) of B₁₂ cofactors. The Cartesian coordinates of all optimized structures used in the current work can be found in the Supporting Information (Tables ST3–ST11). For each optimized geometry, harmonic frequencies were calculated to verify that the optimized structure corresponds to a stable minimum. In all cases the stable minimum was confirmed.

2.1. Structural and Electronic Properties of Methylcobalamin Cofactor. The initial target of our investigation was a truncated model of methylcobalamin (Figure 1), which contains a corrin ring with the side chains replaced by H atoms, and in one axial position (lower face) has an imidazole (Im) ligand. The other axial position (upper face) is occupied by a methyl group. As expected, the optimized structure of the Im–[Co^{III}(corrin)]–Me⁺ provides a reliable description of both axial bond lengths in MeCbl (Table 1). In particular, the optimized Co–C bond distance of 1.968 Å as well as the Co–N axial bond length of 2.132 Å reasonably agree with X-ray values of 1.979(4) and 2.162(4) Å, respectively.³¹ The results of present DFT/BP86 analysis are also in accord with axial bond lengths reported by the previous theoretical calculations.^{17,25–27,29}

To further characterize the truncated model of MeCbl, a potential energy curve that corresponds to Co–C bond homolytic dissociation was determined where the optimized structure of Im–[Co^{III}(corrin)]–Me⁺ was used as a reference (Supporting Information Figure SF1). Starting from the minimum at 1.968 Å, the Co–C bond length was systematically increased by 0.05 Å up to 3.6 Å, and, at each point, geometry optimization was carried out with constraint imposed on the Co–C distance. For distances that exceeded the value of 3.6 Å, only very small energy changes were observed, and by extrapolation we estimated that the cleavage should be essentially completed around 4.2 Å. The Co–C bond dissociation energy (BDE) was also computed based on the energy difference between the fully optimized structure of Im–[Co^{III}(corrin)]–Me⁺ and its separate fragments. The BDE computed this way has a value of 42.0 kcal/mol, whereas the zero point energy (ZPE) correction is equal to 5.0 kcal/mol. Thus, the ZPE corrected dissociation energy for MeCbl, 37.0 kcal/mol (see Table 2), is consistent with experimental values of 37 ± 3 and 36 ± 4 kcal/mol based on thermolysis¹² and employing calorimetric³² measurements, respectively.

The changes of spin density caused by the Co–C bond elongation were also extracted from DFT calculations (Supporting Information Figure SF1, lower panel). Only spin densities associated with the cobalt and carbon atom of the methyl group were analyzed because changes on the other atoms were less significant. We were not able to obtain an unrestricted singlet solution with polarized spins for distances shorter than 2.65 Å, which is consistent with a similar analysis reported for

TABLE 2: The Energetics and Thermodynamic Data Corresponding to Axial Ligand Dissociation^a

reaction	ΔE^b (kcal/mol)	ZPE correction (kcal/mol)	ΔE (PCM) ^c (kcal/mol)	ΔH^d (kcal/mol)	$\Delta S(\Delta S_{\text{trans}})^d$ (eu)	ΔG°^d (kcal/mol)
Im-[Co ^{III} (corrin)]-Me ⁺ = Im + [Co ^{III} (corrin)]-Me ⁺	16.5	1.5	9.4	16.4	41.6(38.1)	4.0
[Co ^{III} (corrin)]-Me ⁺ = [Co ^{II} (corrin)] ⁺ + •Me	43.0	4.8	44.8	44.2	44.2(33.9)	31.2
Im-[Co ^{III} (corrin)]-Me ⁺ = Im-[Co ^{II} (corrin)] ⁺ + •Me	37.0	5.0	41.1	38.4	45.3(34.0)	24.9
Im-[Co ^{III} (corrin•)]-Me = Im + [Co ^{III} (corrin•)]-Me	8.2	1.3	3.9	8.1	41.8(38.1)	-4.4
Co ^{III} (corrin•)-Me = Co ^I (corrin) + •Me	20.4	3.0	21.3	21.2	38.7(33.9)	9.7
Im-[Co ^{III} (corrin•)]-Me = Im + Co ^I (corrin) + •Me	28.6 ^e	4.3	25.2	29.3	80.5(72.0)	5.3

^a Obtained at the BP86/6-31G(d) level of theory. ^b ZPE corrected. ^c The energetics for PCM model with dielectric constant for water as a solvent. ^d The thermodynamic data were calculated with the assumption of validity of the ideal gas law. ^e The energetics correspond to the sum of the values for the two upper reactions.

a truncated model of coenzyme B₁₂.³⁰ This pattern of spin density changes indicates that the diradical character of the cofactor does not appear until the Co-C separation reaches a value of greater than 2.65 Å, and the full diradical character is developed when the Co-C bond is stretched to ~3.2 Å.

2.2. Structural and Electronic Properties of the One-Electron Reduced Methylcobalamin Cofactor. The structure of the Im-[Co^{III}(corrin)]-Me⁺, along with the potential energy curve, suitably reproduces the essential features of MeCbl. This finding strengthens our confidence that electronic and structural properties of the anion radical species (for which structural data is not available) would be reasonably well predicted by DFT/BP86 calculations. One should note that the parent MeCbl molecule is neutral, whereas its reduced analogue, [MeCbl]^{•-}, has a negative charge. Because the truncated structure (Figure 1, bottom panel) does not have the negative phosphate-containing side chain, the truncated Im-[Co^{III}(corrin)]-Me⁺ model is singly charged, and the reduced analogue is thus neutral. However, the truncation of the nucleotide loop that contains the phosphate group does not affect the electronic properties of the Co-C bond as was recently demonstrated in the case of coenzyme B₁₂.^{26b}

The initial structure of reduced cofactor was generated from the truncated Im-[Co^{III}(corrin)]-Me⁺ model by addition of an extra electron. Its geometry optimization was carried out by assuming a doublet electronic state, and stability of the structure was verified by frequency calculations. The analysis of spin density distribution shows that the one-electron reduced cofactor can be best characterized as a corrin π radical, which is denoted as Im-[Co^{III}(corrin•)]-Me to emphasize that the additional electron is almost entirely localized on the corrin ring. The comparison of geometrical parameters shows that its structure is not significantly different from that of the neutral complex and that addition of an electron has only minor influence on axial bond lengths. More specifically, the Co-C bond shortens from 1.968 to 1.958 Å, and a similar shortening from 2.132 to 2.112 Å is also noticed for the Co-N_{Im} distance (Table 1). A similar trend of slightly shorter Co-C and Co-N_{Im} bonds (generally less than 0.1 Å) in reduced species, with a small increase in the positive charge on the cobalt atom, has been noticed by Pratt and van der Donk²⁸ for reduced vinylcobalamins. In another DFT study employing the B3LYP functional, Birke et al.¹⁰ found that one-electron reduction had no effect (± 0.01 Å) on the Co-C distance in a MeCbl model similar to that of Figure 1, regardless of base-off or base-on. Very little change of the corrin structure was observed, which is consistent

with the notion that the structure of corrin ring is very robust and is influenced only by the nature of axial ligands.

To establish how the properties of [MeCbl]^{•-} are affected by removal or by exchange of an axial base, geometry optimization was carried out for two other structural models; one was without axial base, and the other was with the imidazole ligand replaced by water. Spin density distribution in the reduced species was not affected by removal or exchange of the axial base. The length of the Co-C bond shows sensitivity to axial base changes, and the lack of the axial base causes a shortening of this bond to 1.932 Å. To get further insight into electronic properties of these corrin π -radicals, the Kohn-Sham orbitals located near the HOMO-LUMO gap were extracted from DFT calculations. Figure 2 shows their energy levels as well as the location of two orbitals essential for Co-C bond rupture; the first one is associated with the corrin ring (π^*_{corrin} in red), and the second is the antibonding sigma of the Co-C bond ($\sigma^*_{\text{Co-C}}$ in blue). The point of particular interest is the change of the orbital energies when the axial ligand varies from no-base \rightarrow H₂O \rightarrow Im. In all three models the location of the SOMO, which is π^*_{corrin} relative to HOMO-1, remains unaffected by the nature of the axial base. On the other hand, for the $\sigma^*_{\text{Co-C}}$ orbital, a dramatic dependence on coordination state is observed. This orbital in Im-[Co^{III}(corrin•)]-Me lies ~1.5 eV above the SOMO for the base-off complex, and for [Co^{III}(corrin•)]-Me it is only ~0.5 eV higher in energy. This dramatic change is caused by removal of the N-donor axial ligand. In the case of an H₂O axial ligand the energy gap is somewhere between these two cases discussed above. This particular sensitivity can be readily explained if one takes into account that the $\sigma^*_{\text{Co-C}}$ orbital has not only antibonding character with respect to the cobalt (d_{z^2}) and carbon (p_z) orbitals but that it also has antibonding character with respect to the axial base (p_z). The participation of these atomic orbitals can be depicted as³³ $\sigma^*_{\text{Co-C}} \approx -c_1\phi - [N(p_z)] + c_2\phi[\text{Co}(d_{z^2})] - c_3\phi[\text{C}(p_z)]$, and therefore removal of the axial ligand or the presence of a weaker base simply diminishes its double antibonding character. This also implies that lengthening of the Co-N_{ax} bond may effectively reduce the energy gap between these electronic states that have dominant π^*_{corrin} and $\sigma^*_{\text{Co-C}}$ character.

3. Results and Discussion

3.1. Co-C Bond Dissociation in [MeCbl]^{•-}. The central issue of the present study is the question of how the dissociation energy of the Co-C bond is lowered upon the one-electron

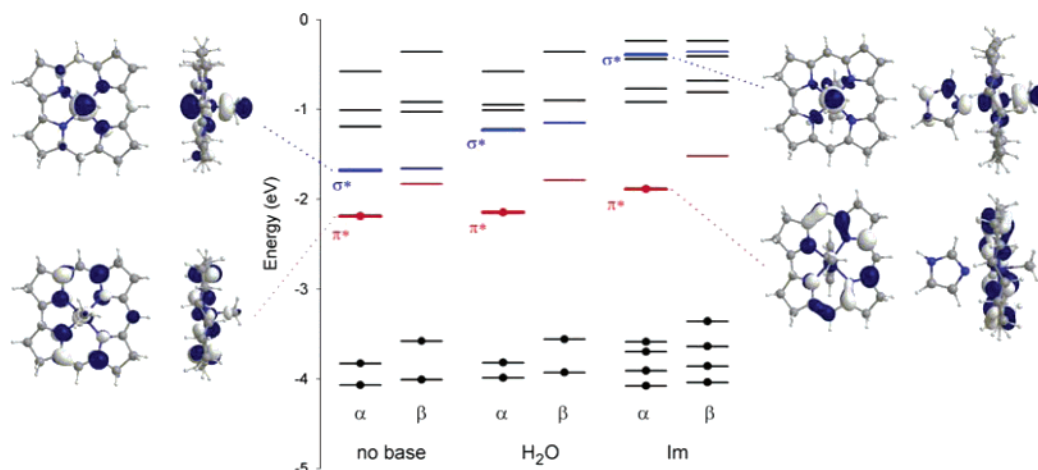
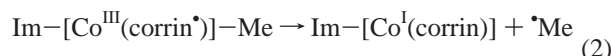
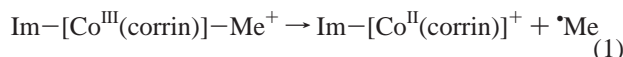


Figure 2. Energy diagram representing orbitals for B-[Co^{III}(corrin*)]-Me (B = no base, H₂O, or Im).

reduction. To address this computationally, dissociation energies have been estimated as follows:



The first equation refers to the Co-C cleavage in the neutral MeCbl cofactor and does not require any further analysis. To obtain the Co-C dissociation energy of Im-[Co^{III}(corrin*)]-Me, the Co-C bond was repeatedly elongated with a step of 0.05 Å, and the geometry was reoptimized at each point. However, we were not able to correctly dissociate the Co-C bond that leads to formation of a methyl radical. Instead, the DFT calculations showed early displacement of the axial base when the Co-C bond was elongated. As concluded before, the lengthening of Co-N_{ax} may effectively reduce the energy gap between these two states. To quantify such energy lowering, the TD-DFT method was applied to obtain a manifold of excited states along the cobalt-imidazole stretched coordinate (Figure 3). The lowest π^*_{corrin} state is affected very little by changes in the Co-N_{ax} length, and the same holds for other excited states with the exception of the state which has $\sigma^*_{\text{Co-C}}$ dominant character. Near the equilibrium it lies ~1.6 eV above the π^*_{corrin} , but its energy steeply decreases when the separation between cobalt and imidazole increases. After crossing two other excited states, at ~2.25 and ~2.35 Å, respectively, it becomes the lowest excited state. To obtain these energy curves it was necessary to interpolate some solutions (marked by open circles) because the single-reference based TD-DFT/BP86 method does not behave properly near the degeneracy. Similar calculations have been carried out for H₂O-[Co^{III}(corrin*)]-Me⁺ (Supporting Information Figure SF2). In case of the latter, the replacement of Im by H₂O initially lowers the energy of the $\sigma^*_{\text{Co-C}}$, but additional lowering is caused by the H₂O-Co bond elongation.

Consequently, the best candidates for reactive complexes are either base-off corrin π -radicals or six-coordinate species with an elongated Co-N_{ax} bond. Thus, the base-off reduced complex, which has the smallest $\pi^*_{\text{corrin}}-\sigma^*_{\text{Co-C}}$ energy gap, was given special attention in further analysis. To obtain the dissociation energy, the geometry optimization was first carried out along the Co-C stretch to verify that the complex [Co^{III}(corrin*)]-Me can dissociate properly to form a methyl radical. The energy curve near the Co-C distance of 2.3 Å was not as

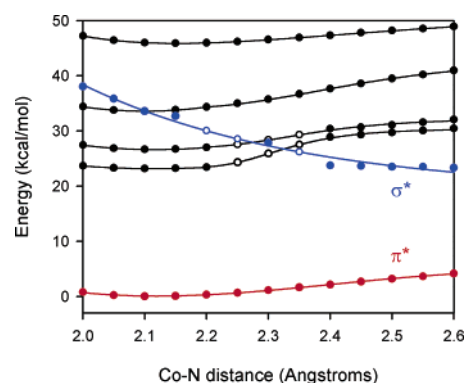


Figure 3. Low-lying excited states of Im-[Co^{III}(corrin*)]-Me computed as a function of Co-N distance.

smooth as desirable, but at larger distances the energy change was monotonic, and the behavior was systematic. Independently, the dissociation energy of 20.4 kcal/mol was estimated as a difference of the fragments (Table 2). To explore what causes the energy lowering and why the energy curve shows some irregularities, the low-lying excited states of [Co^{III}(corrin*)]-Me were computed using the TD-DFT/BP86 approach along the Co-C distance (Figure 4). The TD-DFT method behaves problematically when the SOMO-LUMO energy gap gets very small. Therefore, for Co-C distances between 2.2 and 2.4 Å the electronic excitations have been interpolated.³⁴

The most important feature of the reductive cleavage mechanism is the involvement of two electronic states. The initial [Co^{III}(corrin*)]-Me state has dominant π^*_{corrin} character, but as the Co-C bond is stretched the unpaired electron moves to the $\sigma^*_{\text{Co-C}}$ state, and the final cleavage involves [Co^{II}(corrin)]-Me. The significant BDE reduction is due to the shift of the unpaired electron (formally ascribed to cobalt) between the $\pi^*_{\text{corrin}}-\sigma^*_{\text{Co-C}}$ states along the elongated Co-C coordinate. This leads to homolytic cleavage that finally involves a three-electron (σ)²(σ^*)¹ bond (Figure 4).

The analysis of spin density changes provides further insight into the reductive cleavage mechanism. The spin densities associated with the corrin ring, the cobalt, and the methyl carbon were extracted from each optimized structure along the Co-C distance (Figure 4b). At equilibrium the unpaired electron is primarily localized on the corrin with noticeable spin density present on Co (~0.07), which may reduce the bond strength. When the Co-C bond is stretched to 2.3 Å, rather dramatic changes are observed, and a crossing of all three spin density curves takes place. Changes in spin density along the Co-C

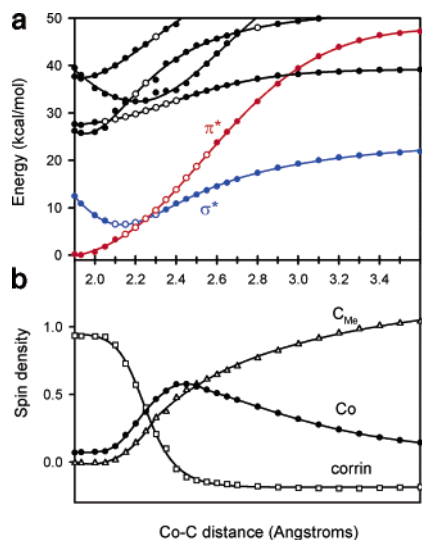


Figure 4. (a) The upper panel shows the low-lying electronic states of $[\text{Co}^{\text{III}}(\text{corrin}^*)]\text{-Me}$ computed as a function of Co-C distance. (b) The lower panel shows spin density changes in $[\text{Co}^{\text{III}}(\text{corrin}^*)]\text{-Me}$ along the Co-C stretch.

coordinate in the radical (Figure 4b) nicely reflect the energy curves depicted in Figure 4a. Spin density shift from the corrin into the methyl, accompanying the Co-C bond dissociation, appears to be a two-stage process. Initial dramatic changes correspond to intramolecular $\pi^*_{\text{corrin}}-\sigma^*_{\text{Co-C}}$ shifts. The maximum spin population on cobalt of ~ 0.6 occurs at a Co-C distance of ~ 2.4 Å, just as the system leaves the “crossing” and as the ground state changes its character from π^*_{corrin} to $\sigma^*_{\text{Co-C}}$. At this point, spin on the corrin drops from its original value of ~ 1 to nearly 0, and virtually all spin is localized in the axial Co-C system (the odd electron in the $\sigma^*_{\text{Co-C}}$ orbital). Upon further elongation of the Co-C bond in the σ^* state, less intense changes are observed; spin on the methyl carbon rises asymptotically to ~ 1 at the expense of the spin on cobalt. It is evident from Figure 4b that some spin polarization between the cobalt and the corrin will persist in the Co^{I} product. This finding is consistent with previous DFT calculations where an open-shell singlet spin state was obtained³⁵ and, in accordance with a CASPT2 study, indicates that this complex may have some admixture of Co^{II} (d^7) character.³⁶

Whether the Co-C cleavage can be viewed as homolytic or heterolytic depends upon formal localization of the unpaired electron in the $\sigma^*_{\text{Co-C}}$ state of the radical. Such assignments are somewhat arbitrary. For example, a description such as $\text{Co}^{\text{II}}\text{-Me}$ implies that the odd electron is localized on the cobalt, and the cleavage should be described as homolytic because the common electron pair from the $\text{Co}^{\text{II}}\text{-Me}$ moiety would be equally distributed between dissociated fragments. On the other hand, if we assume that the unpaired electron is located on the carbon, which corresponds to a $\text{Co}^{\text{III}}\text{-Me}^-$ configuration, then the cleavage would be regarded as heterolytic. However, if the unpaired electron is equally shared between cobalt and carbon, the Co-C cleavage cannot be so easily described as homolytic or heterolytic. This is the most likely case, and only a formal assignment can be made. The usual assignment of the unpaired electron to cobalt is supported by the spin density distribution, which indicates that the unpaired electron is closer to the cobalt atom in the σ^* state when the Co-C distance is not large. Because of this we will refer to the Co-C cleavage as homolytic.

3.2. Comparison with Thermodynamic and Kinetic Data. Mechanisms involving two electronic states have been found

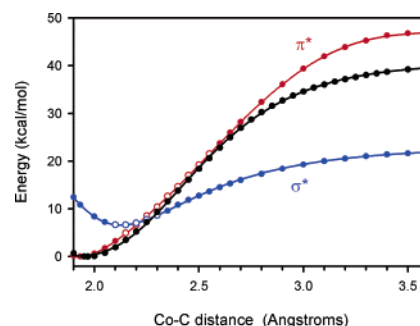


Figure 5. Comparison of energy dissociation curves for neutral (black) and reduced (red and blue) forms of MeCbl cofactor. The energies of neutral and reduced forms have been plotted with respect to a minimum energy that is assumed to be zero in both cases.

to be very efficient in both intramolecular or intermolecular dissociative electron-transfer reactions of organic radical anions^{37–42} or DNA single strand breaks⁴³ where the π^* state crosses the dissociative σ^* state at the avoided crossing. These electronic states are uncoupled by symmetry, and the coupling occurs by a symmetry-breaking coordinate. However, there is a substantial difference between the present work (as summarized in Figure 5) and the above-mentioned reactions where the $\pi^*-\sigma^*$ crossing determines a transition state (energy maximum along the reaction path) for bond rupture. In the present case, the $\sigma^*_{\text{Co-C}}$ electronic state (Figure 5) is not truly repulsive, or dissociative. In fact, it has an energy minimum at a Co-C distance of ~ 2.1 Å, and the energy of the products is higher than the energy of the $\pi^*_{\text{corrin}}-\sigma^*_{\text{Co-C}}$ intersection (Figure 5). Consequently, after the $\pi^*_{\text{corrin}}-\sigma^*_{\text{Co-C}}$ crossing, additional energy is needed for the Co-C bond to break. Hence, the BDE is not determined by the state avoided crossing but rather by the difference between the energy of the $\sigma^*_{\text{Co-C}}$ electronic state at infinite Co-C distance and the energy minimum of the π^*_{corrin} state. This energy, which is 20.4 kcal/mol for $[\text{Co}^{\text{III}}(\text{corrin}^*)]\text{-Me}$, can be compared directly to 37.0 (Table 2) kcal/mol in $\text{Im-}[\text{Co}^{\text{III}}(\text{corrin})]\text{-Me}^+$, which leads to a bond strength reduction of $\sim 55\%$.

The most energetically efficient reductive cleavage is from the base-off species (Table 2), whereas the Co-C bond cleavage from six-coordinated complexes follows the departure of the axial base. The energy required for axial base displacement is difficult to assess and varies substantially with experimental conditions. The experimental ΔH for dissociation of the intramolecular DBI ligand from neutral MeCbl in aqueous solution, as determined by Brown et al.,⁴⁴ is in the range of 6.49–7.65 kcal/mol, depending on ionic strength. However, the ΔH values for dissociation of an N-methylimidazole axial base from $\text{MeCbi}(\text{N-Im})^+$ ⁴⁵ are 3.1 and 6.9 kcal/mol in aqueous solution and in ethylene glycol, respectively.⁴⁶ In the case of MeCbl, the most reliable computational estimation of DBI binding energy, predicted at 7.5 kcal/mol, has been reported by Rovira et al.^{26a} and was obtained based on the full structure of the cofactor. Our estimation for the imidazole displacement in case of the truncated $\text{Im-}[\text{Co}^{\text{III}}(\text{corrin})]\text{-Me}^+$ structure gives 16.5 kcal/mol, and the inclusion of solvation energies (using a PCM approach) brings this value to 9.4 kcal/mol (Table 2). Approximately half of this value, 8.2 kcal/mol, is obtained for reduced $\text{Im-}[\text{Co}^{\text{III}}(\text{corrin}^*)]\text{-Me}$ species, and only 3.9 kcal/mol is obtained upon solvation (Table 2). Interestingly, although the Co- N_{ax} bond is slightly shorter in the reduced form, the dissociation energy required for displacement of the axial base is $\sim 50\%$ lower than in the case of MeCbl.

The DFT-based thermodynamic results provide additional insight with respect to the base-on/base-off species. Although the entropic contribution is essentially the same for all reactions depicted in Table 2 (with obvious exception for the last one where two bonds are cleaved), the corresponding free-energies are very different. The Co–C bond dissociation is largely entropy driven,⁴⁷ but the overall ΔS is not much larger than translational ΔS_{transl} ⁴⁸ (Table 2). Accordingly, one can expect that the entropy will mainly rise after the Co–C bond is essentially broken, so the energetic barrier must be nearly surmounted before the large entropy increase occurs. In the case of the one-electron reduction of Im–[Co^{III}(corrin)]–Me⁺ the ΔG° for imidazole displacement changes from 4.0 to –4.4 kcal/mol, and the latter would be even lower when solvent effects are taken into consideration. This implies that the base-off form should prevail, which is the reverse of what could be predicted from ΔE alone. Given all the simplifications, one can cautiously assume that the two forms of the reduced species will exist at least in comparable amounts and in rapid equilibrium, which would agree well with estimates made by Birke et al.¹⁰ The situation is clearly different for Co–C bond homolysis of the neutral cofactor where the dominant base-on form has lower dissociation energy rather than the base-off form.

The ΔH^\ddagger value of 18.9 kcal/mol, derived by Lexa and Savéant⁷ from temperature dependence of the rate constant cleavage for MeCbl•⁴⁵ in a 1:1 DMF–propanol mixture, leads to a Co–C BDE of ~17 kcal/mol, after a viscous flow correction. The latter can be directly compared with our computed value of 20.4 kcal/mol for [Co^{III}(corrin•)]–Me. The agreement is satisfactory, which suggests that the BP86/6-31G-(d) level of theory is reliable. We believe the comparison is valid in view of weak solvent dependence of the ΔH values for Co–C bond cleavage as apparent from Table 2. Because the Co–N_{ax} bond is absent in the products of Co–C homolysis in [MeCbl]•[–], its energy (or the difference between Co–N_{ax} and Co–O BDEs) should be added to the BDE of MeCbl•, not subtracted as was done by Martin and Finke in footnote 77 of ref 12. As a result, one would obtain $\text{BDE}([\text{MeCbl}]^{\bullet-}) = \Delta H^\ddagger_{\text{r}}(\text{MeCbl}^\bullet) + \text{BDE}(\text{C–N}_{\text{Im}}) - \Delta H^\ddagger_{\text{r}}$, which is ~20 kcal/mol as opposed to the 12 kcal/mol originally proposed.¹² In contrast to our findings, considerably lower ΔH^\ddagger values of 5.8 and 7.6 kcal/mol (depending on a solvent) were determined by Birke and co-workers.¹⁰ The homolysis of [MeCbl]•[–] was measured in a DMF–methanol mixture, that is, in solvent very similar to the original conditions of Lexa and Savéant.⁷ To estimate the Co–C BDE value, Birke and co-workers¹⁰ did not use their ΔH^\ddagger values; instead, they considered relevant thermodynamic cycles, which required some assumptions in regard to the unavailable ΔS values. As a result, a Co–C BDE value of 13 kcal/mol was obtained, which is in apparent agreement with the 12 kcal/mol estimate of Martin and Finke.¹² The mechanism proposed by Birke et al.¹⁰ involves Co–C bond cleavage as a pre-equilibrium (characterized by an equilibrium constant of ~0.1 M) followed by rate-determining dissociation of the caged product complex. These authors assumed that distinct free energy minimum associated with the product complex should exist, which implies that the energy of the $\pi^*_{\text{corrin}}-\sigma^*_{\text{Co-C}}$ intersection would determine the fast rate for Co–C dissociation within the solvent cage. To reconcile this scheme with the thermodynamically estimated BDE of 13 kcal/mol, an unreasonably large enthalpic barrier for product separation is needed. In contrast, our DFT calculations suggest that the energy for Co–C bond breaking within the solvent cage (in solution) will constitute most of the overall energy barrier for formation of

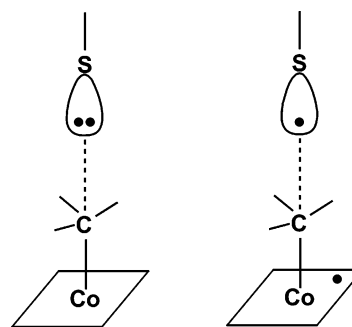


Figure 6. Comparison of closed-shell (left) with the open-shell singlet (right) configurations for the reaction involving methyl transfer between thiolate and base-off MeCbl.

free products from the base-off reduced species. As noted above, the correspondence between our DFT computed Co–C BDE value for the base-off reduced species of ~20.4 kcal/mol and the experimental ΔH^\ddagger value of 18.9 kcal/mol for [MeCbl]•[–]^{7a} stands in support of this argument.

3.3. Relevance to Biological Systems. The significant lowering of energy that is required for the Co–C bond cleavage suggests that the electron-transfer (ET) associated with the [MeCbl]•[–] species may be relevant to the B₁₂ enzymatic catalysis. In principle, this can be sufficient to explain the rate enhancement observed in B₁₂-dependent enzymes. Nevertheless, the ET has not been considered as a plausible mechanism for any AdoCbl-dependent or MeCbl-dependent enzymes,^{12,49} and several arguments have been presented against this hypothesis. The most critical argument is that biological reducing agents are not sufficiently strong to overcome the very negative reduction potentials for B₁₂ cofactors. This is based on the assumption that a reducing agent, such as an Fe–S cluster,⁵⁰ has to be present near B₁₂ cofactor to facilitate outer-sphere ET, which would then initiate the formation of methyl or adenosyl radicals available for follow-up processes. However, without any strong reducing agent near the B₁₂ cofactor, species such as [MeCbl]•[–] may be formed in the presence of substrate (nucleophile) via substrate-to-MeCbl ET within the reactant complex. In such an alternative mechanistic proposal the intermediates in catalytic cycles of these enzymes may have electronic structure similar to reduced forms of B₁₂ cofactors, and anion–radical-like [MeCbl]•[–] species may be transiently formed during catalytic turnover.

In case of methionine synthase, which catalyzes methyl transfer from MeCbl to homocysteine, both the methyl transfer to cob(I)alamin and the demethylation of the resulting MeCbl are generally believed to proceed by an S_N2 mechanism. The S_N2 mechanism implies that elementary Co–C bond cleavage would be heterolytic and that the cobalt will alternate between Co^{III} and Co^I oxidation states in catalytic cycle.^{2,3} Using a structural model of base-off MeCbl cofactor, [Co^{III}(corrin)]–Me⁺, and a model of homocysteine substrate, MeS[–], the involvement of species such as [MeCbl]•[–] may be postulated as follows: the S_N2 nucleophilic substitution requires that an electron pair residing on sulfur be formally transferred as a pair and shared with the carbon atom. At the same time, upon heterolytic cleavage of the Co–C bond, the square-planar Co^I (d⁸) intermediate would be formed. Under this assumption, the reaction should proceed through a transition state in which the Co–CH₃ bond is partially broken, and a new bond between CH₃ and S is partially formed. The reactant complex associated with this type of reaction (Figure 6, left configuration) would be described by a closed-shell wavefunction as has been assumed by Jensen and Ryde.⁵¹ However, there is also the

possibility that the reactant complex would have a diradical character, such as $[\text{Co}^{\text{III}}(\text{corrin}^{\bullet})]-\text{Me}\cdots^{\bullet}\text{SMe}$, and its electronic configuration would be described as an open-shell singlet (Figure 6). The diradical state will be promoted by the presence of high-lying MOs, which belongs to MeS^{\bullet} , and will have energies very close to π^*_{corrin} . In this reactant complex (Figure 6, right configuration), the corrin moiety bears resemblance to the one-electron reduced species described in this work. Consequently, the initial step of the methyl transfer reaction would involve homolytic cleavage of the Co–C bond of anion radical, followed by formation of a methyl radical that will eventually combine with the $^{\bullet}\text{SMe}$ radical to produce the same product complex as in the case of $\text{S}_{\text{N}}2$ substitution. Thus, the reaction would be best described as methyl (radical) transfer to yield the same product complex as in the case of $\text{S}_{\text{N}}2$ substitution. It is worth noting that the appearance of $[\text{MeCbl}]^{\bullet-}$ can be associated with a substrate-to-MeCbl ET within the reactant complex, which is induced by the presence of substrate. This proposal is fundamentally different to what was described as single electron transfer (SET) by Matthews.² In the SET mechanism the initial step involves homolytic cleavage of the Co–C bond followed by electron transfer from Me–homocysteine radical complex to cobalamin without involvement of the anion–radical-like $[\text{MeCbl}]^{\bullet-}$ form of the MeCbl cofactor.

Although the full analysis of methyl transfer reaction mechanisms mediated by methylcobalamin is beyond the scope of present work, the question arises as to whether an electronic configuration with polarized spins can be energetically more stable than the corresponding one with paired electrons (Figure 6). To test this hypothesis, the MeS^{\bullet} substrate was placed at a C \cdots S distance of 4.0 Å and the energy was computed at DFT/BP86, assuming both closed-shell and open-shell wavefunction. The open-shell singlet UHF solution gives a lower energy by 4.4 kcal/mol and a value of $\langle S^2 \rangle = 0.46$, which indicates that the cofactor–substrate complex has multi-configurational character, with spin density polarized between the S and the corrin ring.

4. Concluding Remarks

This study is among first few^{10,11,28} in which DFT calculations have been applied to investigate electronic and structural properties of one-electron reduced cobalt corrinoids. In particular, the DFT/BP86 level of theory has been applied to explore the mechanism of reductive Co–C bond cleavage in MeCbl. The most important outcome of the present analysis is the finding that significant lowering of dissociation energy is due to involvement of two electronic states (Figure 5). The initial state is described as a corrin π -radical, but during Co–C bond breaking the unpaired electron moves to the $\sigma^*_{\text{Co}-\text{C}}$ state, and the final dissociation involves a three-electron $(\sigma)^2\sigma^*$ bond.

The results of the present DFT analysis were compared to thermodynamic and to kinetic data available from electrochemical measurements. The reasonable agreement between our calculated BDE values for model complexes and experimental BDEs for $[\text{MeCbl}]^{\bullet-}$ and MeCbl^{\bullet} indicates that the dissociation kinetics is determined primarily by the BDEs, not by the $\pi^*_{\text{corrin}}-\sigma^*_{\text{Co}-\text{C}}$ intersection. The computed values agree better with the older data of Lexa and Sav  ant^{7a} rather than those of Birke and co-workers¹⁰ for reasons explained in Section 3. However, our conclusion regarding the base-off reduced species as the reactive form is more consistent with the recent work of Birke et al.¹⁰ With respect to reduced base-off species, we presented thermodynamics arguments based on enthalpy and entropy analysis for the fast kinetics observed.

We also suggested the possible connection of present work with B_{12} enzymatic catalysis and the involvement of anion–radical-like $[\text{MeCbl}]^{\bullet-}$ species in cobalamin-dependent methyl transfer reactions. Our proposal does not require the presence of any strong reducing agent near the cofactor, but rather substrate-induced formation of anion–radical-like species as a part of the reactant complex. Preliminary calculations indicate that the electronic configuration with polarized spins, where one electron is located on the corrin ring, is energetically lower than the corresponding configuration with paired spin. This finding offers a mechanistic alternative to classical $\text{S}_{\text{N}}2$ reaction that has been most frequently invoked in the case of methionine synthase. It has been known for some time that such ET/bond rupture mechanisms greatly enhance the reaction rates in comparison to $\text{S}_{\text{N}}2$ reactions, as has been discussed in the literature by Marcus,⁵² Shaik et al.,⁵³ and Sav  ant.⁵⁴

Supporting Information Available: The relevant structural parameters, electronic energies, spin densities for the reduced species and Cartesian coordinates of the optimized structures generated by the study. This material is available free of charge via the Internet at <http://pubs.acs.org>.

References and Notes

- (1) See for example: (a) B_{12} ; Dolphin, D. Ed.; Wiley-Interscience: New York, 1982. (b) Banerjee, R. *Chem. Biol.* **1997**, *4*, 175–186. (c) Ludwig, M. L.; Matthews, R. G. *Annu. Rev. Biochem.* **1997**, *66*, 269–313. (d) *Vitamin B₁₂ and B₁₂ Proteins*; Kr  utler, B., Arigoni, D., Golding, B.T. Eds.; Wiley-VCH: New York, 1998. (e) Marzilli, L.G. in *Bioinorganic Catalysis* Reedijk, J., Bouwman, E. Eds.; Marcel Dekker: New York, 1999; pp 423–468. (f) Banerjee, R. *Chemistry and Biochemistry of B₁₂*; John Wiley & Sons: New York, 1999. (g) Toraya, T. *Cell. Mol. Life Sci.* **2000**, *57*, 106–127. (h) Banerjee, R., *Biochem.* **2001**, *40*, 6191–6198. (i) Banerjee, R.; Ragsdale, S. W. *Annu. Rev. Biochem.* **2003**, *72*, 209–247. (j) Banerjee, R. *Chem. Rev.* **2003**, *103*, 2083–2094. (k) Toraya, T. *Chem. Rev.* **2003**, *103*, 2095–2127. (l) Brown, K. L. *Chem. Rev.* **2005**, *105*, 2075–2149. (m) Randaccio, L.; Geremia, S.; J.; Wuerger, J. *Organomet. Chem.* **2007**, *692*, 1198–1215.
- (2) Matthews, R. G. *Acc. Chem. Res.* **2001**, *34*, 681–689.
- (3) The heterolytic cleavage of the Co–C bond to form the methyl carbocation in cobalamin-dependent methyltransferases should not be taken literally; these heterolytic reactions are most likely the nucleophilic displacement of $\text{S}_{\text{N}}2$ -type, and the presence of free carbocations is not involved. Alternative mechanisms have been postulated for methyl transfer including oxidative addition and single electron transfer (see ref 2 for details).
- (4) Halpern, J. *Science* **1985**, *227*, 869–875.
- (5) (a) Finke, R. G.; Hay, B. P. *Inorg. Chem.* **1984**, *23*, 3041–3043. (b) Hay, B. P.; Finke, R. G. *J. Am. Chem. Soc.* **1986**, *108*, 4820–4829. (c) Finke, R. G. In *Vitamin B₁₂ and B₁₂ Proteins*, Lectures presented at the 4th European Symposium on Vitamin B₁₂ and B₁₂ Proteins; Kr  utler, B., Arigoni, D., Golding, B.T., Eds.; Wiley-VCH: Weinheim, Germany, 1998; Chapter 25.
- (6) (a) Hay, B. P.; Finke, R. G. *Polyhedron* **1988**, *7*, 1469–1481. (b) Luo, L. B.; Li, G.; Chen, H. L.; Fu, S. W.; Zhang, S. Y. *J. Chem. Soc., Dalton Trans.* **1998**, 2103–2107.
- (7) (a) Lexa, D.; Sav  ant, J.-M. *J. Am. Chem. Soc.* **1978**, *100*, 3220–3222. (b) Lexa, D.; Sav  ant, J.-M. *Acc. Chem. Res.* **1983**, *16*, 235–243.
- (8) Kim, M.-H.; Birke, R. L. *J. Electroanal. Chem.* **1983**, *144*, 331–350.
- (9) Ohkubo, K.; Fukuzumi, S. *J. Phys. Chem. A* **2005**, *109*, 1105–1113.
- (10) Birke, R. L.; Huang, Q.; Spataru, T.; Gosser, D. K. Jr. *J. Am. Chem. Soc.* **2006**, *128*, 1922–1936.
- (11) Spataru, T.; Birke, R. L. *J. Electroanal. Chem.* **2006**, *593*, 74–86.
- (12) Martin, B. D.; Finke, R. G. *J. Am. Chem. Soc.* **1992**, *114*, 585–592.
- (13) This estimation is based upon the assumption that the reactivity order for reduced species should follow the same order as is observed for neutral MeCbl cofactor with respect to base-on/base-off forms. In fact, recent electrochemical studies and DFT calculations (including the present work) indicate that such order is reversed for reduced complexes. See section 3.2 for a detailed discussion.
- (14) Quantum mechanical calculations at the MP2/6–311G* level of theory suggest that the S–S bond in the dissociative σ^* state of $\text{PhS}^{\bullet}-\text{SPh}^{\bullet}$, should be significantly elongated. See, for details Antonello, S.;

Daasbjerg, K.; Jensen, H.; Taddei, F.; Maran, F. *J. Am. Chem. Soc.* **2003**, *125*, 14905–14916.

(15) Salem, L.; Eisenstein, O.; Anh, N. T.; Bürgi, H. B.; Devaquet, A.; Segal, G.; Veillard, A. *Nouv. J. Chim.* **1977**, *1*, 335–348.

(16) Stich, T. R.; Brooks, A. J.; Buan, N. R.; Brunold, T. C. *J. Am. Chem. Soc.* **2003**, *125*, 5897–5914.

(17) Jaworska, M.; Lodowski, P.; Andruniow, T.; Kozłowski, P. M. *J. Phys. Chem. B* **2007**, *111*, 2419–2422.

(18) (a) Savèant, J.-M. *Acc. Chem. Res.* **1993**, *26*, 455–461. (b) Savèant, J.-M. *Adv. Phys. Org. Chem.* **2000**, *35*, 117–192.

(19) Spataru, T.; Birke, R. L. *J. Phys. Chem. A* **2006**, *110*, 8599–8604.

(20) Spataru and Birke (ref 19) assumed that the length of the Co–C bond for the one-electron reduced species should be substantially elongated in comparison to the neutral cofactor. However, there is no experimental evidence to support this claim, and the low dissociation energy itself is not indicative that the Co–C bond length should be perturbed upon addition of an electron. Furthermore, the results of CASSCF calculations must be further improved by the addition of dynamical correlation, which is usually treated via second-order perturbation theory (CASPT2).

(21) Runge, E.; Gross, E. K. U. *Phys. Rev. Lett.* **1984**, *52*, 997–1000.

(22) (a) Baerends, E. J.; Ricciardi, G.; Rosa, A.; van Gisbergen, S. J. A. *Coord. Chem. Rev.* **2002**, *230*, 5–27. (b) Dreuw, A.; Head-Gordon, M. *Chem. Rev.* **2005**, *105*, 4009–4037. (c) Dreuw, A. *ChemPhysChem* **2006**, *7*, 2259–2274.

(23) (a) Becke, A. D. *J. Chem. Phys.* **1986**, *84*, 4524–4529. (b) Perdew, J. P. *Phys. Rev. B* **1986**, *33*, 8822–8824.

(24) Frisch M. J. et al., *Gaussian 03*, Revision C.02; Gaussian, Inc.: Wallingford, CT, 2004 (for full reference see Supporting Information).

(25) Jensen, K. P.; Ryde, U. *J. Phys. Chem. A* **2003**, *107*, 7539–7545.

(26) (a) Rovira, C.; Biarnes, X.; Kunc, K. *Inorg. Chem.* **2004**, *43*, 6628–6632. (b) Rovira, C.; Kozłowski, P. M. *J. Phys. Chem. B* **2007**, *111*, 3251–3257.

(27) Dölker, N.; Morreale, A.; Maseras, F. *J. Biol. Inorg. Chem.* **2005**, *10*, 509–517.

(28) Pratt, D. A.; van der Donk, W. J. *Am. Chem. Soc.* **2005**, *127*, 384–396.

(29) Kuta, J.; Patchkovskii, S.; Zgierski, M. Z.; Kozłowski, P. M. *J. Comput. Chem.* **2006**, *27*, 1429–1437.

(30) Kozłowski, P. M.; Kamachi, T.; Toraya, T.; Yoshizawa, K. *Angew. Chem., Int. Ed.* **2007**, *46*, 980–983.

(31) (a) Randaccio, L.; Furlan, M.; Geremia, S.; Slouf, M.; Srnova, I.; Toffoli, D. *Inorg. Chem.* **2000**, *39*, 3403–3413. (b) Randaccio, L.; Geremia, S.; Nardin, G.; Wuerger, J. *Coord. Chem. Rev.* **2006**, *250*, 1332–1350.

(32) Hung, R. R.; Grabowski J. J. *J. Am. Chem. Soc.* **1999**, *121*, 1359–1364.

(33) Andruniow, T.; Kuta, J.; Zgierski, M. Z.; Kozłowski, P. M. *Chem. Phys. Lett.* **2005**, *410*, 410–416.

(34) The single-reference TD-DFT method is not capable of providing any detailed description when the crossing of two curves take place. Only an estimate can be obtained based on energy interpolation. However, the analysis of vertical excitations outside of this range provides a clue as to which states should be connected, and therefore the overall picture is not affected by such interpolation.

(35) Jensen, K. P.; Ryde, U. *ChemBioChem* **2003**, *4*, 413–424.

(36) Jensen, K. P. *J. Phys. Chem. B* **2005**, *109*, 10505–10512.

(37) Lorange, E. D.; Kramer, W. H.; Gould, I. R. *J. Am. Chem. Soc.* **2002**, *124*, 15225–15238.

(38) Laage, D.; Burghardt, I.; Sommerfeld, T.; Hynes, J. T. *ChemPhysChem* **2003**, *4*, 61–66.

(39) (a) Laage, D.; Burghardt, I.; Sommerfeld, T.; Hynes, J. T. *J. Phys. Chem. A* **2003**, *107*, 11271–11291. (b) Burghardt, I.; Laage, D.; Hynes, J. T. *J. Phys. Chem. A* **2003**, *107*, 11292–11306.

(40) Takeda, N.; Poliakov, P. V.; Cook, A. R.; Miller, J. R. *J. Am. Chem. Soc.* **2004**, *126*, 4301–4309.

(41) Costentin, C.; Robert, M.; Savèant, J.-M. *J. Am. Chem. Soc.* **2004**, *126*, 16051–16057.

(42) Antonello, S.; Maran, F. *Chem. Soc. Rev.* **2005**, *34*, 418–428.

(43) Simons, J. *Acc. Chem. Res.* **2006**, *39*, 772–779.

(44) Brown, K. L.; Peck-Siler, S. *Inorg. Chem.* **1988**, *27*, 3548–3555.

(45) Cbi stands for cobinamide. The MeCbi⁺ species has the same charge as [Co^{III}(corrin)]–Me⁺.

(46) Sirovatka-Dorweiler, J.; Matthews, R. G.; Finke, R. G. *Inorg. Chem.* **2002**, *41*, 6217–6224.

(47) Our DFT calculations provided $\Delta S = 33.9$ eu for Co–C bond dissociation in [Co^{III}(corrin*)]–Me, which is in general agreement with the large, positive estimates of ΔS by Birke and co-workers¹⁰ and also with $\Delta S^\ddagger = 21 \pm 3$ eu for Co–C bond breaking in [MeCbi]^{•+},¹² resulting from Lexa and Savèant's kinetic data.^{7a}

(48) The Sakur-Tetrode equation may give ΔS_{transl} values that are too large in aqueous solution; see for example Amzel, L. M. *Proteins: Struct., Funct., Genet.* **1997**, *28*, 144–149.

(49) Finke, R. G.; Martin, B. D. *J. Inorg. Biochem.* **1990**, *40*, 19–22.

(50) According to Finke and co-workers (refs 12 and 49) the presence of a relatively strong reducing agent such as an Fe–S cluster is still insufficient to reduce B₁₂ cofactors.

(51) Jensen, K. P.; Ryde, U. *J. Am. Chem. Soc.* **2003**, *125*, 13970–13971.

(52) Marcus, R. A. *J. Phys. Chem. A* **1997**, *101*, 4072–4087.

(53) Shaik, S. S.; Schlegel, H. B.; Wolfe, S. *Theoretical Aspects of Physical Organic Chemistry. The S_N2 Mechanism*; Wiley-Interscience: New York, 1992.

(54) Costentin, C.; Robert, M.; Savèant, J.-M. *J. Am. Chem. Soc.* **2004**, *126*, 16834–16840.